QP351 .J65
Mai
NPL
433331

STIC-ILL

From: Lacourciere, Karen
Sent: Tuesday, February 25, 2003 5:58 PM
To: STIC-ILL
Subject: ill order

Please provide the following references for use in examining 09/853,895

Anesthesiology (Hagerstown), (1996) Vol. 84, No. 5, pp. 1205-1214.

Journal of Neuroscience (1996), 16(23), 7407-7415

Neuroscience Research (Shannon, Ireland) (1999), 33(2), 111-118

Society for Neuroscience Abstracts, (2001) Vol. 27, No. 1, pp. 416. print.

Anesthesiology (2001), 94(6), 1010-1015

NeuroReport (2001), 12(15), 3251-3255

European Journal of Pharmacology, (March 31, 2000) Vol. 392, No. 3, pp. 141-145.

Thank-you!

Karen A. Lacourciere Ph.D.
CM1 11D09 GAU 1635
(703) 308-7523

pp. 7407-7415 (9) The Journal of Neuroscience, December 1, 1996, 16(23):7407–7415

Cloning and Characterization of Postsynaptic Density 93, a Nitric Oxide Synthase Interacting Protein

Jay E. Brenman, Karen S. Christopherson, Sarah E. Craven, Aaron W. McGee, and David S. Bredt

Department of Physiology and Programs in Biomedical Sciences and Neuroscience, University of California at San Francisco School of Medicine, San Francisco, California 94143-0444

Nitric oxide (NO) formation in brain is regulated by the calcium/calmodulin dependence of neuronal NO synthase (nNOS). Calcium influx through NMDA-type glutamate receptors is efficiently coupled to nNOS activity, whereas many other intracellular calcium pathways are poorly coupled. To elucidate possible mechanisms responsible for this coupling, we performed yeast two-hybrid screening to identify proteins that interact with nNOS. Two nNOS interacting proteins were identified: the postsynaptic density proteins PSD-93 and PSD-95. Here, we report the cloning and characterization of PSD-93. PSD-93 is expressed in discrete neuronal populations as well as in specific non-neuronal cells, and it exhibits complex molecular diversity attributable to tissue-specific alternative splicing. PSD-93, like PSD-95, binds to nNOS and to the NMDA receptor 2B. PSD-93, however, is unique among PSD-95/SAP-90 family members in its expression in Purkinje neuron cell bodies and dendrites. We also demonstrate that the PDZ domain at the N terminus of nNOS is required, but it is not sufficient for interaction with PSD-93/95. Given that PSD-93 and PSD-95 each contain multiple potential binding sites for nNOS and the NMDA receptor, complexes involving oligomers of PSD-93/95 may help account for the functional as well as the physical coupling of nNOS to NMDA receptors.

Key words: neuronal nitric oxide synthase; NMDA receptor; postsynaptic density; Purkinje neurons; glutamate; calcium

Nitric oxide (NO) functions as a messenger molecule in numerous neuronal pathways in brain and periphery (Bredt and Snyder, 1992; Vincent and Hope, 1992; Garthwaite and Boulton, 1995). NO formation in neurons is stimulated by increases in intracellular calcium that locally activate neuronal NO synthase (nNOS) through interaction with calmodulin (Garthwaite et al., 1988; Bredt and Snyder, 1989; Knowles et al., 1989; Bredt and Snyder, 1990). Intracellular calcium is tightly regulated in neurons, and only certain calcium influx pathways are efficiently coupled to nNOS activity. In cerebellar granule cells, calcium influx through NMDA-type glutamate receptors is coupled to nNOS activity and to subsequent accumulation of cGMP (Ferrendelli et al., 1974; Bredt and Snyder, 1989; Garthwaite et al., 1989). This NMDA receptor pathway demonstrates specificity. Other neurotransmitters that increase intracellular calcium in granule neurons, including kainate, quisqualate, AMPA, and muscarinic agonists, are not as effective at stimulating NO formation (Kiedrowski et al., 1992). Depolarizing agents effectively stimulate NO formation in brain, but this increase is largely blocked by AP5 (Raiteri et al., 1991), a specific NMDA receptor antagonist. NMDA receptor antagonists also attenuate basal and stimulated NO levels in brain of awake animals (Luo et al., 1993). A fundamental understanding of NO actions in brain requires elucidation of mechanisms that functionally couple nNOS to NMDA receptors.

Received July 8, 1996; revised Sept. 4, 1996; accepted Sept. 9, 1996.

This work was supported by grants from the National Science Foundation, National Institutes of Health, the Lucille P. Markey Charitable Trust, the Chicago Community Trust, the McKnight Endowment Fund for Neuroscience, and the Esther A. and Joseph Klingenstein Fund to D.S.B. We thank Paul Ulrich for assistance with sequence alignments.

Correspondence should be addressed to Dr. David S. Bredt, Department of Physiology, University of California at San Francisco School of Medicine, 513 Parnassus Avenue, San Francisco, CA 94143-0444.

Recently, NMDA receptor subunits have been shown to bind to the postsynaptic density protein PSD-95 (Kornau et al., 1995). The physiological significance of NMDA receptor interaction with PSD-95 is unclear but is postulated to play a role in the assembly of multiprotein complexes involved in NMDA receptor-mediated synaptic plasticity (Kornau et al., 1995).

To determine which protein–protein interactions participate in coupling NMDA receptors to NO formation in brain, we screened for nNOS binding proteins using the yeast two-hybrid system (Fields and Song, 1989). We identified two classes of interacting gene products from a screen of 10^6 plasmids (Brenman et al., 1996). One group encoded fragments of PSD-95, and the other group encoded a novel related protein, PSD-93. Here, we report the cloning and characterization of PSD-93. We find that PSD-93 mRNA is highly enriched in brain, where it occurs discretely in specific neuronal populations. Outside the brain, PSD-93 occurs in specific neuronal and non-neuronal cells. Cloning of multiple PSD-93 cDNAs from brain indicates molecular heterogeneity, consistent with tissue-specific alternative splicing of the mRNA. Immunocytochemistry demonstrates that PSD-93 is likely postsynaptic in cerebellar Purkinje cell dendrites but does not rule out a presynaptic localization elsewhere. Biochemical studies demonstrate that the PDZ motifs within PSD-93 bind to nNOS as well as to the tSXV motif of NMDA receptor 2B. Surprisingly, we find that additional sequence outside the PDZ domain of nNOS is required for binding to PSD-93/95.

MATERIALS AND METHODS

Generation of PSD-93 and PSD-95 antiserum. Glutathione-*S*-transferase fusion proteins encoding amino acids 77–453 of PSD-93 and amino acids 1–386 of PSD-95 were expressed and purified from *Escherichia coli*. Guinea pigs were immunized with the PSD-93 fusion, and rabbits were immunized with the PSD-95 fusion. Antigens were emulsified in complete and incomplete Freund's adjuvant. Serum bleeds were evaluated by ELISA.

cDNA cloning and analysis. A human PSD-93 cDNA encoding amino acids 116–421 isolated as an nNOS interacting fragment was used to screen a rat brain cDNA library (Stratagene, La Jolla, CA). Ten hybridizing cDNAs were isolated from a screen of 10^6 phage. Clones were sequenced on both strands using the dideoxy chain termination method (U.S. Biologicals). The GenBank accession number for PSD-93 is U50717.

mRNA isolation and Northern blot analysis. RNA was isolated using the guanidine isothiocyanate/CsCl method, and mRNA was selected using oligo-dT Sepharose. For Northern blotting, mRNA was separated on a formaldehyde agarose gel and transferred to a nylon membrane. The filter was sequentially hybridized with random-primed ^{32}P probes that were generated using PSD-93 cDNAs as template. The common probe corresponded to nucleotides 237–927 of PSD-93. Transcript specific probes, 5′a and 5′b, were generated by the polymerase chain reaction and corresponded to the unique regions 5′ of lysine 14 (see Fig. 1*B*). After each hybridization, the membrane was washed at high stringency, 68°C, with 0.1% SSC, 0.1% SDS, and exposed to x-ray film at −70°C.

In situ hybridization. Adult rats were perfused with 4% paraformaldehyde, and brains were harvested, post-fixed at 4°C for 3 hr, and cryoprotected in 20% sucrose overnight. Twenty micrometer sections were cut on a cryostat and melted onto glass slides (Plus, Fisher Scientific, Houston, TX). Embryonic day 15 rats were delivered by Cesarean section, fixed in paraformaldehyde, and processed in parallel with adult brain. *In situ* hybridization used ^{35}S-labeled RNA probes as described (Sassoon and Rosenthal, 1993). Antisense probe to PSD 93 (nucleotides 237–927) and sense control were synthesized from pBluescript vectors. Tissue sections were exposed to x-ray film for 4 d and then were dipped into photographic emulsion (Kodak NTB-2) and exposed for 14 d.

Immunohistochemistry. Sprague Dawley rats were anesthetized with pentobarbital and perfused with 4% freshly depolymerized paraformaldehyde in 0.1 M phosphate buffer. Tissues were removed and post-fixed in paraformaldehyde for 1 hr at 4°C. Tissues were cryoprotected overnight in 20% sucrose. Free-floating sections (40 μm) were cut on a sliding microtome. Sections were blocked for 1 hr in PBS containing 1.5% normal goat serum and then incubated overnight in the same buffer containing diluted antiserum. For indirect immunofluorescence, secondary goat anti-rabbit FITC- and donkey anti-guinea pig Cy-3-conjugated antibodies were used according to the manufacturer's specifications (1:200; Jackson Laboratories, Bar Harbor, ME).

Fusion-protein affinity chromatography. Fusion protein of GST fused to amino acids 77–453 of PSD-93 or amino acids 1–100, 1–150, or 1–195 of nNOS were expressed in *E. coli* and purified on glutathione-Sepharose beads as described (Brenman et al., 1995). Whole brain was homogenized in 10 vol (w/v) Tris-HCl buffer, pH 7.4, and centrifuged at 32,000 × *g* for 20 min. Membranes were solubilized for 2 hr at 4°C in buffer containing 200 mM NaCl and 1% Triton X-100, and insoluble material was pelleted by centrifugation at 100,000 × *g* for 30 min. Solubilized membranes were incubated with control (GST) or GST fusion-protein beads. Samples were loaded into disposable columns, which were washed with 50 vol of buffer containing 1% Triton X-100 + 300 mM NaCl. Retained proteins were eluted with 150 μl of loading buffer and resolved by SDS-PAGE. Blots were hybridized with a monoclonal antibody to nNOS (Transduction Laboratories, Lexington, KY). NMDA receptor peptide (KLSSIESDV) or control peptide (KLSSIEADA) was added where indicated during tissue incubation with the fusion protein.

RESULTS

Molecular cloning of PSD-93

To determine the molecular structure of PSD-93, we screened a rat brain library with a fragment of human PSD-93 isolated as an nNOS interacting gene product (Brenman et al., 1996). Ten hybridizing clones were isolated from a screen of 10^6 phage. Clones encoding the full open-reading frame were sequenced on both strands and predicted a protein of 834 amino acids and 93 kDa (Fig. 1*A*). Sequence analysis revealed that PSD-93 shares ~70% homology with PSD-95 (or SAP-90) and with HDLG (or SAP-97). These three proteins share a common domain structure consisting of three PDZ (or GLGF) protein motifs followed by an SH-3 domain and finally a domain homologous to yeast guanylate kinase. Considerable sequence divergence between these homologous proteins occurs at the N terminus. In addition, HDLG and PSD-93 have small inserts between the SH3 and guanylate kinase domains. PSD-93 also has a unique larger insert between the second and third PDZ repeats.

Analysis of multiple PSD-93 cDNAs indicated three sites for putative alternative splicing. Certain cDNA clones isolated from the library had either a 102 base pair (bp) (34 amino acid) or a 45 bp (15 amino acid) insert between amino acids K624 and R625 (Fig. 1*C*). Another example of alternative splicing was found by RT-PCR amplification of rat brain cDNA using primers that flank the large insert that is unique to PSD-93. In these amplifications, we consistently found two bands, one corresponding to the PSD-93 clones isolated from the library and another that lacked 156 nucleotides (52 amino acids) between PDZ-2 and PDZ-3 (noted as a deletion in Fig. 1*D*).

The greatest degree of heterogeneity was found at the N terminus of PSD-93 where we isolated cDNA clones with four distinct sequences (Fig. 1*B*). The most commonly obtained transcript, 5′b, contained an inframe starter ATG codon that predicted a protein of 93 kDa and contained 220 bp of 5′ untranslated sequence. The largest transcript, 5′a, diverged from 5′b immediately upstream of lysine 14, encoded two potential starter methionines, and contained at least 257 bp of 5′ untranslated sequence. The sequence of two other cDNAs isolated from the library diverged from PSD-93 at points further into the translated sequence. 5′c diverged upstream of alanine 69 and contained an inframe starter methionine. 5′d diverged from the common PSD-93 sequence upstream of threonine 78 and did not contain an inframe ATG start codon. Translation of the 5′d transcript may initiate at the first in frame ATG codon, which occurs at amino acid 228, or may initiate at a noncanonical start codon.

Expression of PSD-93 mRNA

We evaluated the overall distribution of PSD-93 by Northern blotting using a probe to sequences that are present in all of the alternatively spliced forms. PSD-93 mRNA occurred as a single band of ~7.5 kb in poly(A^+) RNA from brain (Fig. 2*A*). Under these conditions, PSD-93 could not be detected in poly(A^+) RNA from kidney, spleen, liver, heart, or skeletal muscle. We also evaluated the distribution of PSD-93 in various brain regions. Highest levels were found in cerebral cortex and cerebellum, with somewhat lower densities in striatum and hippocampus, and essentially no PSD-93 could be detected in brain stem. The PSD-93 hybridizing bands in forebrain regions migrated as ~7.5 kb bands, whereas that in cerebellum migrated just slightly faster (Fig. 2*B*).

The altered migration of PSD-93 mRNA in cerebellum raised the possibility that the message is alternatively spliced in a tissue-specific manner. To evaluate this, we rehybridized the blot with probes corresponding to the two large alternative N termini. The first probe, 5′a, hybridized to a single band of ~7.5 kb from rat brain RNA and resembled the distribution of the general PSD-93 probe in various brain regions (Fig. 2*C*). On the other hand, hybridization with 5′b indicated that this transcript occurs selectively in forebrain regions and is absent from cerebellum (Fig. 2*D*).

We next evaluated the cellular distribution of PSD-93 mRNA by *in situ* hybridization. As reported previously (Brenman et al., 1996), PSD-93 occurred in subpopulations of neurons in the adult brain. In the forebrain, PSD-93 was apparent in cerebral cortex, striatum, and hippocampus. Highest densities in hippocampus were found in pyramidal neurons of Ammon's horn and in granule cells of the dentate gyrus (Fig. 3*a*). In the hindbrain, PSD-93 was restricted to Purkinje neurons of cerebellum (Fig. 3*a*). PSD-93

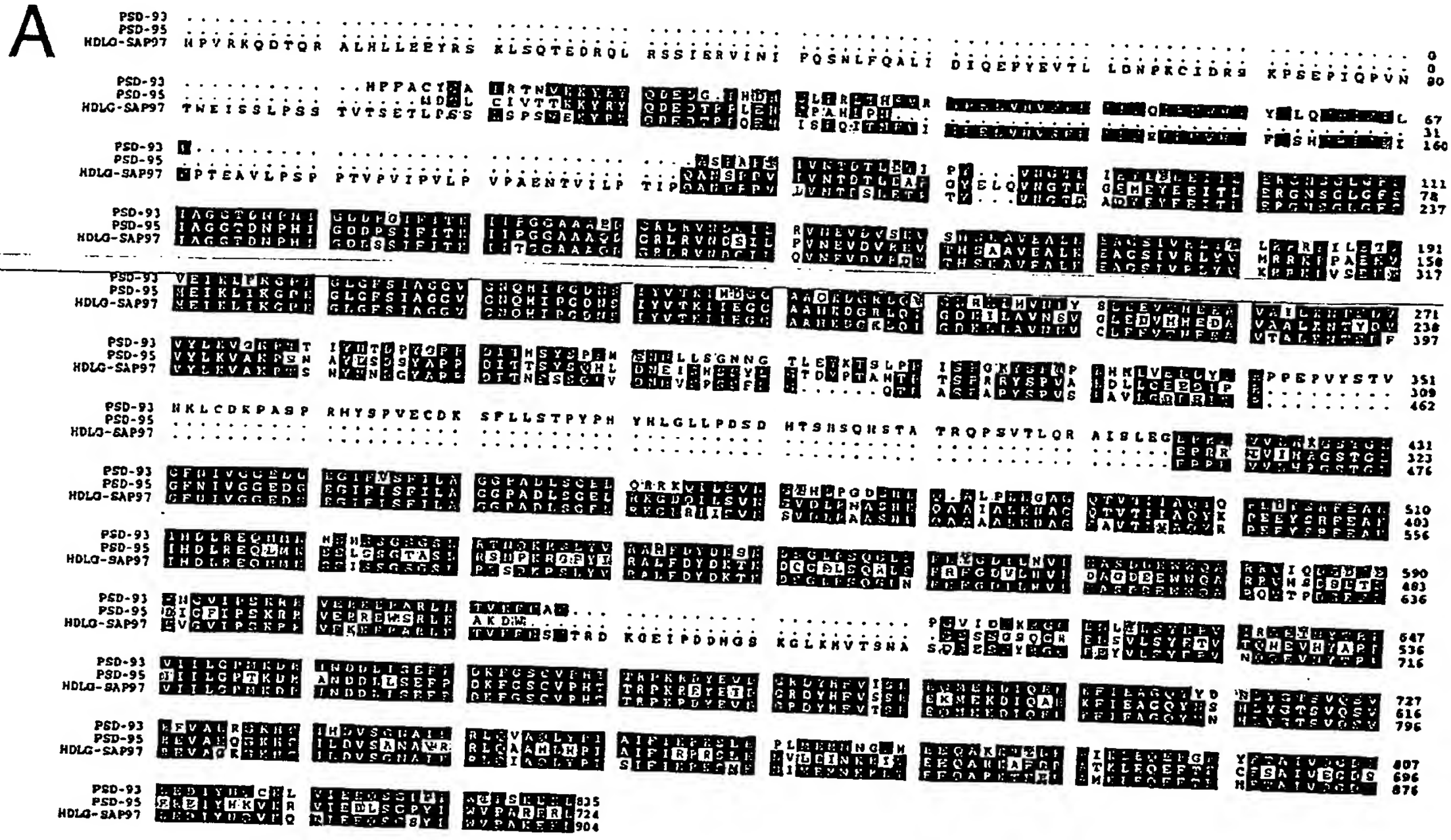

Figure 1. Predicted amino acid sequence and alternative splicing of PSD-93. *A*, Alignment of PSD-93 with PSD-95 and HDLG-SAP97 indicates an overall amino acid identity of ~70%. Identical amino acids are indicated by *black boxes*, and conserved amino acid changes are shaded by *gray boxes*. *B*, The N terminus of PSD-93 is alternatively splice prone. Sequences of the four alternative N-terminal transcripts (5'a–d) are indicated. *Black triangles* denote the sites at which the sequences diverge from PSD-93. The amino acid *numbers* in *bold* refer to that predicted using 5'b of PSD-93. In-frame starter methionines or stop codons are indicated. *C*, Two different alternatively spliced inserts occur between amino acids K624 and R625. The *arrow* indicates the location at which the two isoform insertions occur. The sequences of the alternative insertions are also shown. *D*, A schematic model showing the domain structure of PSD-93. Identified sites of putative alternative splicing are indicated. (PSD-93 has been given GenBank accession number U50717.)
Figure continues.

was not detected in brain stem structures, confirming the regional distribution found by Northern analysis.

To determine expression of PSD-93 in peripheral tissues, we conducted *in situ* hybridization on E15 rat embryo (Fig. 3*b*). We found highest densities of PSD-93 in developing brain and spinal cord. Several neuronal populations in the periphery also showed strong hybridization, including myenteric neurons of the intestine and sensory neurons of the dorsal root ganglia and trigeminal ganglia. Unlike PSD-95, certain non-neuronal tissues contained PSD-93. Particularly high levels of PSD-93 were noted in several glands, including the adrenal, thymus, and submandibular glands.

PSD-93 is present in Purkinje cell bodies and dendrites in cerebellum

To compare the cellular localization of PSD-93 and PSD-95 in brain, we developed affinity-purified antisera to PSD-93 and PSD-95 in guinea pig and rabbit, respectively. Immunoblotting of total brain homogenate demonstrates that antiserum to PSD-93 predominantly recognizes a protein product that migrates at ~103 kDa (Fig. 4). The antiserum to PSD-95 recognizes a protein that migrates at ~95 kDa. Longer exposure of the PSD-95 Western blot reveals a second reactive band of ~75 kDa. This lower band has been noted previously by others (Cho et al., 1992).

Although PSD-95 is postsynaptic in forebrain (Hunt et al., 1996), PSD-95 immunoreactivity in cerebellum is most concentrated in the presynaptic axon terminals of basket cells (Kistner et al., 1993; Hunt et al., 1996). These PSD-95-rich terminals form dense structures called beards or pinceaus about the Purkinje neuron axon hillock (Fig. 5). PSD-93 immunoreactivity, in contrast, is highly enriched in Purkinje neuron somata and dendrites (Fig. 5), suggesting possible postsynaptic functions for PSD-93 in cerebellum. PSD-93 immunoreactivity is also postsynaptic in the dendrites of hippocampal neurons (data not shown). No immunoreactivity is observed with preimmune serum for either PSD-95 or PSD-93.

nNOS binds to PSD-93

PSD-93 was identified in a yeast two-hybrid screen as an nNOS interacting protein (Brenman et al., 1996). To verify this interaction biochemically, we expressed and purified a fragment of PSD-93 as a glutathione-*S*-transferase protein (G-P93) in *E. coli*. The expressed fragment encoded amino acids 77–453, which represent the first two PDZ domains of PSD-93. We evaluated binding of endogenous nNOS to this fragment of PSD-93 by affinity chromatography (Brenman et al., 1996). Crude solubilized brain extracts were incubated with G-P93 or control. Glutathione-Sepharose was added, and nonspecific proteins were removed by washing with buffer containing 300 mM NaCl and 1% Triton

B

5′a

tccccacccctcgttctcttgggaagacagaccccgagacgcactgtacttgccggca
gcagtgcttgccactaggctcggggatggctgcaccaggcgcaggggcagcgatcacagctgccgctcggtctaggctgtctaggcaggctgtcgctccg
agcactgggtgagcaccgagttccggttccccccagcaagctgccactgccgcagcccaaaaggaatgtcccctgttcttaaggaccctgactgttttacacca

atg att tgc cac tgc aaa gtt gct tgc acc aac aac act ttg tcg ttg atg ttt gga tgc aag aag tat cga tac...

M I C H C K V A C T N N T L S L M F G C K K Y R Y ...

14

5′b

ctaattgaaattactgggcataatgctat

atatgccaatgagagattctgagctctcactcagtgccttcaagacatgtcgttttgtagtcagaggaaacagggatcaatgcattttcaaactgacagag
gaacggatgctccttagcagcacatgcccaggatcgtgtgtgtggggcttgcgctgtgctgagaagctgatcaccggcccatatgcccctttatttactgca

atg ttc ttt gca tgt tat tgt gca ctc cgg act aac gtg aag aag tat cga tac...

M F F A C Y C A L R T N V K K Y R Y ...

14

5′c

gagtgcttctctaaaacaatgtgaagaagct atg caa cat gcg ttc att ccg gct agc cct gct cct ata att gtc aac...

M Q H A F I P A S P A P I I V N ...

69

5′d

ggcacgagcttcttcacattgttt tag aga agc aat tgt atc cca cag aag ctg ata att ctc agc aca gac act ttg ...

STOP R S N C I P Q K L I I L S T D T L ...

78

C

gca aaa cct ggt gtg att gat tcc aaa cga gga caa gaa gat ctc att ctt tcc...

A K P G V I D S K R G Q E D L I L S ...

616

Insertion 1

ggg tca ttc aat gac aag cgt aaa aag agc ttc atc ttt tca cga aaa ttc cca
G S F N D K R K K S F I F S R K F P

ttc tac aag aac aag gag cag agt gag cag gaa acc agt gat cct gaa
F Y K N K E Q S E Q E T S D P E

Insertion 2

ggg aca tcc cgg tta ggt gac gac ggt tat gga aca aag act ctg
G T S R L G D D G Y G T K T L

D

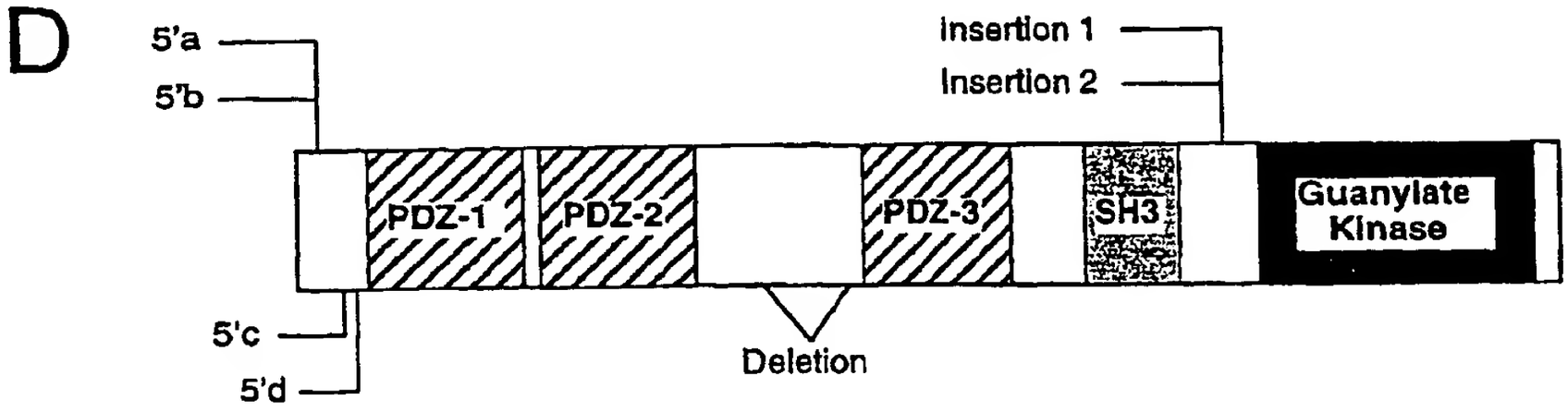

Figure 1 continued.

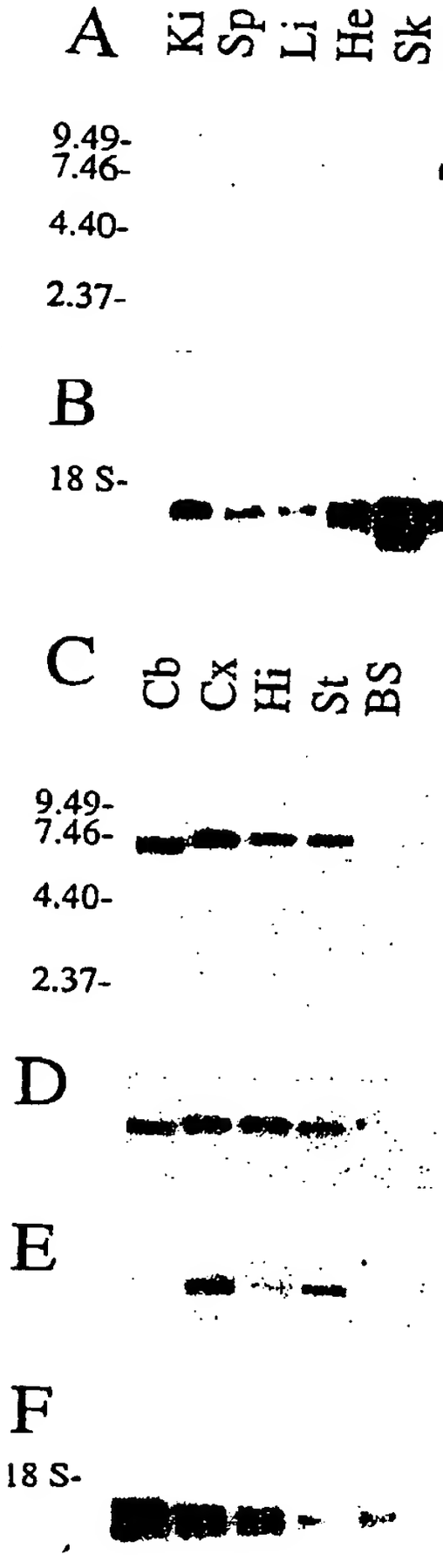

Figure 2. Tissue expression and alternative splicing of PSD-93. *A*, Northern blotting of adult rat tissues indicates that PSD-93 is expressed as an ~7.5 kb transcript that occurs in brain (*Br*) but not in kidney (*Ki*), spleen (*Sp*), liver (*Li*), heart (*He*), or skeletal muscle (*Sk*). *C*, Northern blotting of brain regions demonstrates that PSD-93 is present in cerebellum (*Cb*), cortex (*Cx*), hippocampus (*Hi*), and striatum (*St*) but is absent from brainstem (*BS*). Note that the band in cerebellum migrates slightly faster than that in other brain regions. For *A* and *B*, a probe common to all of the alternatively spliced forms of PSD-93 was used. *D*, *E*, The blot in *B* was sequentially rehybridized with probes corresponding to two of the alternatively spliced N-terminal regions of PSD-93. *C*, Probing with 5′a reveals that the regional distribution of this splice variant is similar to that of PSD-93. *D*, 5′b, however, is selectively absent from cerebellum. *B*, *F*, Duplicate samples of mRNA were probed for glyceraldehyde 3-phosphate dehydrogenase to demonstrate loading and integrity of the mRNA for the above blots.

X-100. Adherent proteins were eluted with loading buffer and resolved by SDS-PAGE. Western blotting showed selective retention of nNOS to a PSD-93 column but not to a control GST column (Fig. 6). Previous studies indicate that nNOS interacts selectively with the second PDZ motif of PSD-95 and that i can be competed away with a peptide corresponding to tl terminal amino acids of the NMDA receptor 2B (KLSSIE To determine whether binding of nNOS to PSD-93 dis similar properties, we repeated the "pull-down" assays presence of varying concentrations of the NMDA recepto tide. We found that this 9-mer peptide potently displaced from PSD-93 (K_d <5 μM). Displacement by the NMDA re peptide was specific. A control peptide (KLSSIEADA), wit point mutations of the consensus serine and valine resid alanines, had no effect on binding, even at higher conc tions (Fig. 6).

The PDZ domain of nNOS is contained within the fir amino acids, whereas the first 195 amino acids of nNOS originally used to identify PSD-93 in a two-hybrid screer therefore asked whether the PDZ domain of nNOS was suf for interaction with PSD-93. To address this question, we neered overlapping constructs spanning the amino termin amino acids of nNOS and screened for interaction with PSD the yeast two-hybrid system (Table 1). We found that cons containing the first 150 amino acids of nNOS were necessar sufficient for association with PSD-95. Deletion of sequenc either side of this 150 amino acid domain produced fusion failed to interact with PSD-93. Importantly, an N-termina amino acid construct encoding the entire consensus PDZ do of nNOS did not associate with PSD-93.

To verify that the PDZ domain of nNOS is not sufficien interaction with PSD-93, we biochemically evaluated bindin ing affinity chromatography. GST fusion proteins encoding a acids 1–100, 1–150, and 1–195 were linked to columr glutathione-Sepharose beads and were incubated with solubi brain extracts (Fig. 7). After the columns were washed, reta proteins were identified by Western blotting. Again, we found amino acids 1–150 of nNOS potently interacted with PSD-9 that amino acids 1–100 are not sufficient for association. In allel experiments, we found that amino acids 1–150 of nNOS necessary and sufficient for interaction with PSD-95 (data shown).

DISCUSSION

These studies identify PSD-93 as a novel member of a gro family of proteins with both PDZ motifs and homology to g ylate kinases. These proteins seem to organize signaling molec at membrane junctions. The PDZ motif contains ~100 an acids and is present in a diverse family of enzymes and struct proteins. The first identified member of this group, discs-l (*dlg*) tumor suppressor protein of *Drosophila*, is localized to tate junctions of epithelial cells in *Drosophila* larvae. The abse of *dlg* in mutant flies results in disruption of the septate juncti loss of cell–cell adhesion, and neoplastic growth of epithelial c in the larval imaginal disks (Woods and Bryant, 1991). Mam lian homologs of *dlg* have also been localized to sites of cell– contact. For example, zona occludens 1 and 2 (ZO1 and ZO occur at tight junctions of epithelial cells (Stevenson et al., 19 Willott et al., 1993; Jesaitis and Goodenough, 1994). PSD SAP-90 and HDLG/SAP-97 are enriched in presynaptic comp ments of certain synapses (Kistner et al., 1993; Lue et al., 19 Muller et al., 1995) and postsynaptic densities of forebrain n rons (Hunt et al., 1996). The high densities of PSD-93 mR identified here in specific neuronal populations in brain periphery suggest an analogous role for PSD-93 in synaptic fu tion. The dramatic enrichment of PSD-93 in cerebellar Purk

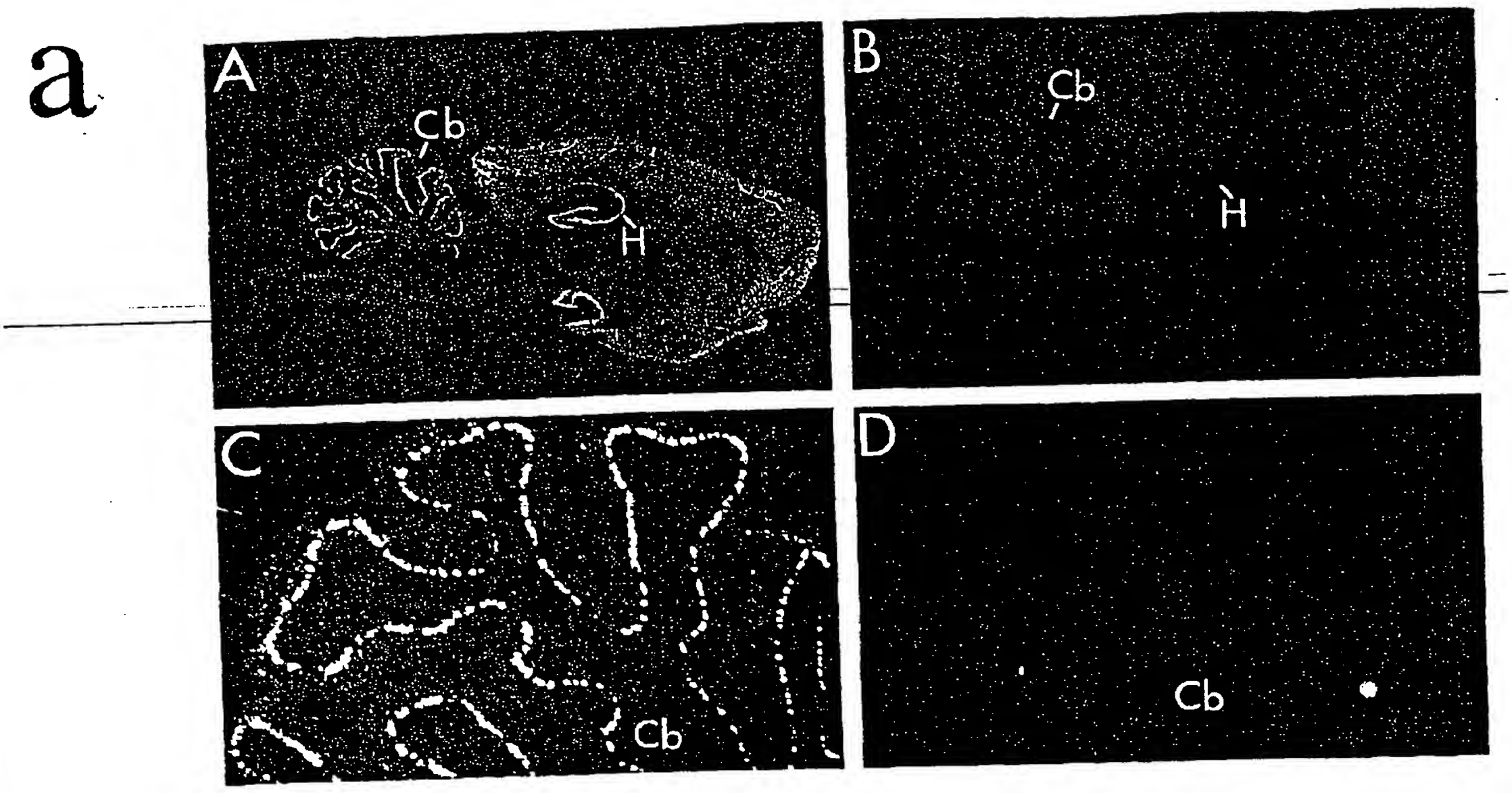

Figure 3. Cellular localization of PSD-93 mRNA in adult brain and E15 embryo. *In situ* hybridization was used to localize transcripts for PSD-93 (*A, C, E, G*) or sense control (*B, D, F, H*). *a*, In adult brain, PSD-93 seems to be neuron-specific and is highly expressed in Purkinje neurons in the cerebellum (*Cb*) and also occurs in pyramidal and granule cells in hippocampus (*H*). *b*, In E15 embryo, PSD-93 is abundantly expressed in neurons of spinal cord (*SC*), dorsal root ganglia (*DRG*), and intestine (*In*). PSD-93 is also observed in cells of the thymus (*Thy*) and submandibular gland (*SG*).

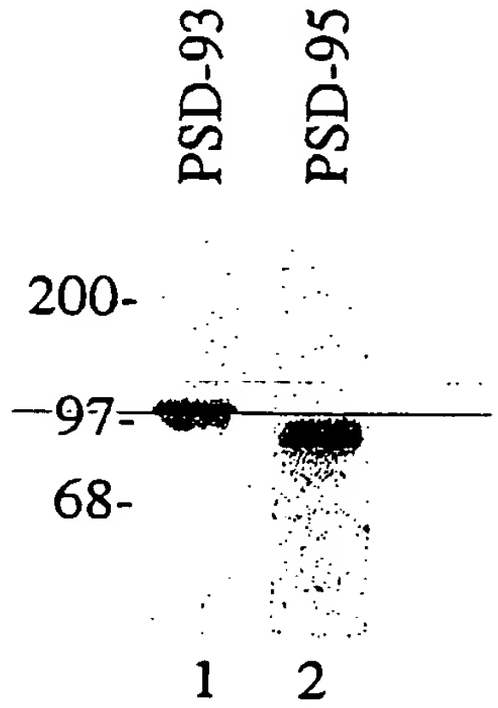

Figure 4. Specificity of antisera to PSD-93 and PSD-95. Western blot analysis reveals that the predominant PSD-93 protein product in rat brain migrates at 103 kDa, whereas the major PSD-95 reactive band migrates at 95 kDa. Crude adult rat brain homogenates (50 μg of protein/lane) were size-fractionated by SDS-PAGE and analyzed by immunoblotting with affinity-purified antiserum to either PSD-93 (*lane 1*) or PSD-95 (*lane 2*). Size markers are in kilodaltons.

cells, which lack other members of this gene family, may indicate an important role for PSD-93 in synaptogenesis for Purkinje cells as well as postsynaptic function in cerebellum. Targeted disruption of PSD-93 *in vivo* should help clarify this question.

PSD-95/SAP-90 was identified independently by two laboratories as an abundant and detergent-insoluble protein enriched in brain synaptosomal fractions (Cho et al., 1992; Kistner et al., 1993). Specific functions for PSD-95 remain uncertain, and no catalytic activity has yet been demonstrated for the guanylate kinase domain. Yeast two-hybrid analysis, however, identified that PSD-95 can bind to NMDA receptor subunits and to certain K^+ channels (Kim et al., 1995; Kornau et al., 1995). PSD-95 and NMDA receptor 2B have been shown to cluster together at synaptic sites in hippocampal neurons in culture (Kornau et al., 1995). In addition, coexpression of PSD-95 with K^+ channel K_v 1.4 results in redistribution and clustering of the channel in cell surface patches (Kim et al., 1995). These studies identified that the first two PDZ repeats of PSD-95 can participate in a domain interaction with ion channels that contain a C-terminal tSXV motif (Kim et al., 1995; Kornau et al., 1995). We similarly find that PSD-93 expressed as a GST fusion protein interacts with K_v 1.4, which contains the tSXV motif (data not shown). Therefore, PSD-93 may also play a role in clustering of synaptic receptors in certain neurons.

In brain, nNOS is enriched in membrane fractions (Hecker et al., 1994; Brenman et al., 1996). Electron micrographic studies demonstrate that membrane-associated nNOS is concentrated in axon terminals and over thick postsynaptic densities (Aoki et al., 1993). This membrane association of nNOS in neurons is mediated by the PDZ-containing domain, because nNOS isoforms lacking this domain occur only in soluble fractions of brain extracts (Brenman et al., 1996). Membrane association of nNOS in brain may be mediated by interaction with PDZ repeats in PSD-95 and PSD-93. These PDZ domain interactions are specific; nNOS interacts selectively with the second PDZ motif of PSD-93/95 (Brenman et al., 1996). Because the first and third PDZ domain of PSD-95 can interact independently with tSXV domains of certain

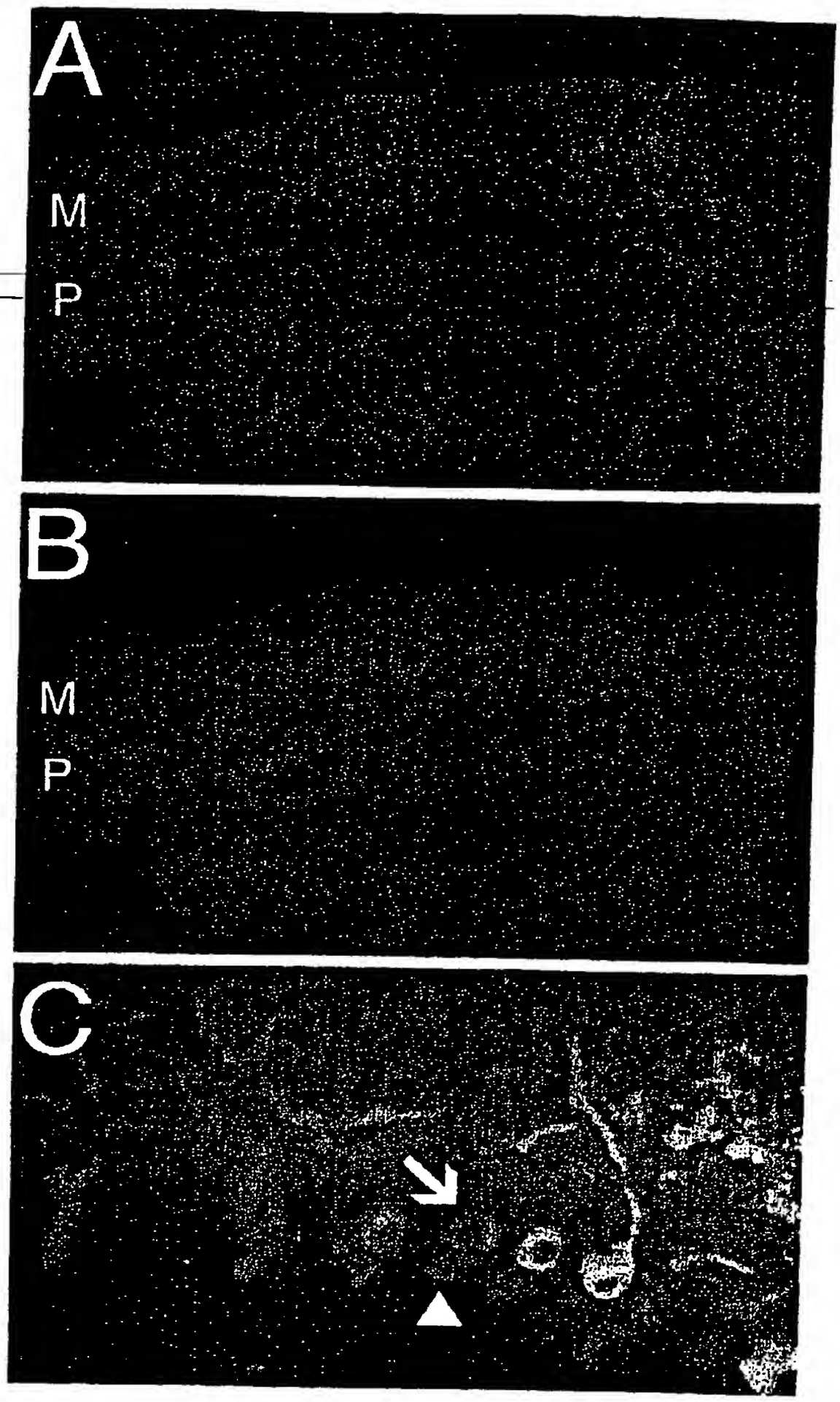

Figure 5. PSD-93 is postsynaptic, whereas PSD-95 is predominantly presynaptic in rat cerebellum. A sagittal section of rat cerebellum was processed for indirect immunofluorescent double-labeling using a guinea pig antiserum to PSD-93 and a rabbit antiserum to PSD-95. *A*, PSD-93 immunoreactivity, visualized in the *red channel*, is present in Purkinje cell somata and molecular layer (*M*) of cerebellum (100× magnification). *B*, PSD-95, visualized in the *green channel*, is present in the synaptic plexus of basket cell axons beneath the Purkinje cell layer (*P*) (100× magnification). *C*, Higher-power double exposure shows that PSD-93 immunoreactivity (*orange*) is confined to Purkinje neurons (*arrow*), whereas PSD-95 immunoreactivity (*green*) primarily labels the presynaptic basket cell pinceaus (*arrowhead*) (400× magnification). Note that the *orange color* observed on double exposure is attributable to the longer exposure times required by FITC filters.

ion channels (Kim et al., 1995; Doyle et al., 1996), PSD-95 and PSD-93 may serve as molecular bridges linking ion channels to nNOS. This compartmentalization of nNOS with ion channels may account for the selective coupling of specific calcium influx

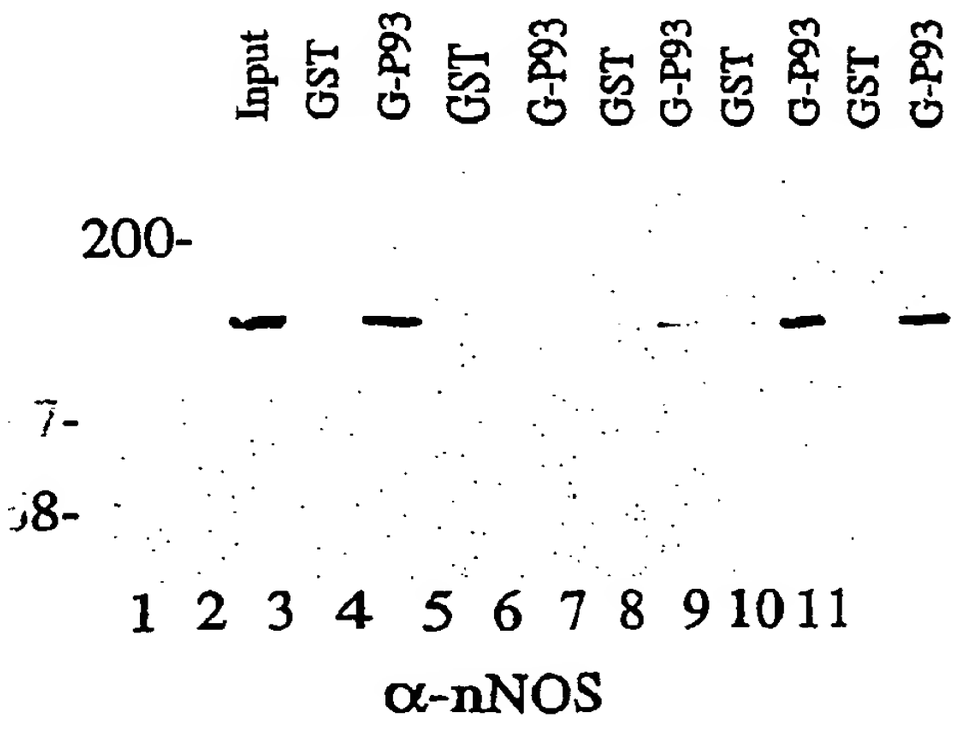

Figure 6. The PDZ repeats of PSD-93 interact with nNOS and the tSXV motif of NMDA receptor 2B. Glutathione-Sepharose beads bound to GST or to a PSD-93 protein fragment (amino acids 77–453) fused to *GST* (*G-P93*) were incubated with brain extracts. After the beads were washed extensively, retained proteins were eluted with 0.2% SDS and separated by SDS/PAGE. Western blotting indicates that nNOS is selectively retained by G-P93 (*lane 3*) but not by GST alone (*lane 2*). Binding assays performed in parallel indicate that an NMDA receptor 2B C-terminal peptide displaces nNOS from G-P93 completely at 10 μM (*lanes 4* and *5*), substantially at 5 μM (*lanes 6* and *7*), and negligibly at 0.1 μM (*lanes 8* and *9*). A control peptide had no effect on nNOS binding to G-P93 at 10 μM (*lanes 10* and *11*). Input = 10% of the protein loaded onto the fusion-protein columns.

pathways to NO formation (Garthwaite, 1991; Raiteri et al., 1991; Kiedrowski et al., 1992).

In central neurons, NO formation is functionally coupled to NMDA receptor activity, and nNOS protein is colocalized with PSD-95 in some, but not all, neuronal populations (Brenman et al., 1996). In cerebellum, an nNOS/PSD-95 complex was identified by immunoprecipitation (Brenman et al., 1996). We have not yet been able to evaluate possible formation of an nNOS/PSD-93 complex in brain membranes, because after affinity purification our antiserum does not immunoprecipitate native PSD-93 protein from brain extracts. Outside the brain, nNOS also occurs in certain neuronal and non-neuronal cell populations, and in many of these peripheral tissues nNOS occurs together with PSD-93. For example, we find that PSD-93 mRNA is enriched in neurons of the myenteric plexus. nNOS also occurs at high densities in myenteric neurons, and NO that is formed in these cells mediates nonadrenergic-noncholinergic relaxation of the intestines (Bult et al., 1990). NMDA receptor activity does not regulate nNOS in the enteric nervous system. Instead, NO formation seems to be linked to calcium influx through ω-conotoxin-sensitive channels (Daniel et al., 1994). It will now be important to determine whether these channels interact with PSD-93 and nNOS in myenteric neurons.

PDZ domains seem to be modular motifs capable of diverse modes of protein–protein interaction. One class of ligands for PDZ domains is the terminal tSXV motif that occurs in certain ion channels and receptors. Recent x-ray crystallography studies of a single PDZ domain demonstrate that the terminal carboxylate group of the tSXV is cradled by the main chain amides as well as an arginine side chain of the PDZ domain (Doyle et al., 1996). In the crystal, the PDZ domain forms a dimer in which the surface of the peptide-binding domain of

Table 1. Interactions of nNOS and PSD-93

Gal4 DNA binding hybrid	Gal4 activation hybrid	β-Galactosidase units
nNOS (amino acids 1–100)	PSD-93 (116–421)	1.23
nNOS (40–150)	PSD-93 (116–421)	1.64
nNOS (40–195)	PSD-93 (116–421)	1.51
nNOS (100–195)	PSD-93 (116–421)	1.06
nNOS (1–150)	PSD-93 (116–421)	14.7
nNOS (1–195)	PSD-93 (116–421)	17.2
Lamin C (66–230)	PSD-93 (116–421)	0.430

Yeast Y187 cells were cotransformed with expression vectors encoding various Gal4 DNA binding domain and Gal4 activation domain fusion proteins. Each transformation mixture was plated on synthetic dextrose plates lacking tryptophan and leucine. Interaction was measured by the liquid culture β-galactosidase assay as described (Fields and Song, 1989; Clonetech).

Values are representative of experiments repeated twice with similar results.

one PDZ subunit interacts with residues in β-strands from the other subunit (Cabral et al., 1996). This binding topology of PDZ domains may explain why the tSXV peptide of NR2B potently blocks nNOS binding to PSD-93.

Other studies have shown that PDZ domains can interact with transmembrane proteins, which entirely lack tSXV motifs (Shieh and Zhu, 1996). Interaction of nNOS with PSD-93/95 shows certain unique characteristics. nNOS is the first peripheral membrane protein found to interact with a PDZ domain. Also, the PDZ domain of nNOS is involved in binding to the PDZ domain of PSD-93/95. Future structural studies of the amino terminal domain of nNOS should identify determinants that confer binding of nNOS to PSD-93/95. Interestingly, we report here that the PDZ domain of nNOS alone is not sufficient for association with PSD-95. It will be important to determine whether interaction of PDZ domains and adjacent sequences is a common mechanism for organization of signaling machinery.

Cloning of PSD-93 identifies a significant heterogeneity of tran-

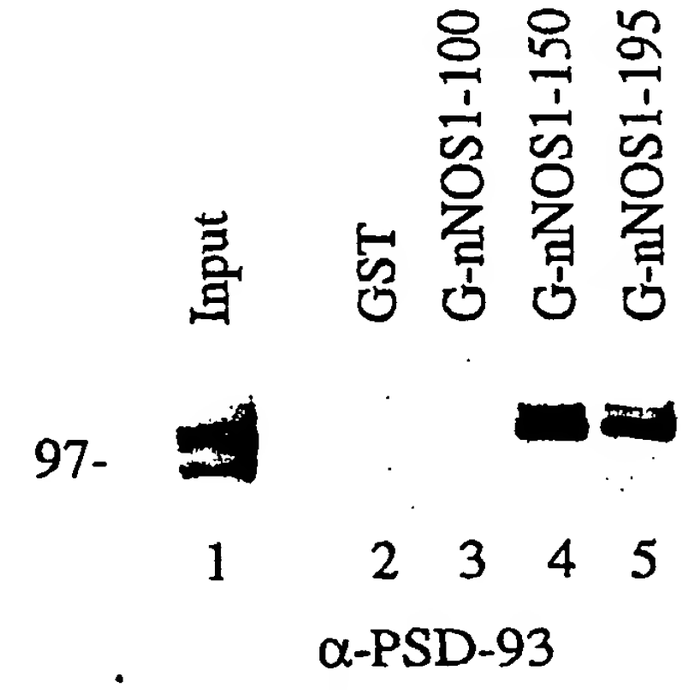

Figure 7. The 100 amino acid PDZ domain of nNOS is not sufficient to bind to PSD-93. Glutathione-Sepharose beads bound to GST alone or to GST fusion-protein fragments encoding various N-terminal domains of nNOS (*G-nNOS*) were incubated with brain extracts. After the beads were washed extensively, retained proteins were eluted with 0.2% SDS and separated by SDS/PAGE. Western blotting with PSD-93 antiserum reveals that PSD-93 does not bind to either *GST* alone (*lane 2*) or to *G-nNOS1-100* (*lane 3*) but is selectively retained by *G-nNOS1-150* (*lane 4*) and *G-nNOS1-195* (*lane 5*). Input = 10% of the protein loaded onto the fusion-protein columns (*lane 1*).

scripts. Our molecular studies identified six examples of putative alternative splicing, and it seems likely that additional heterogeneity exists. Alternative splicing within the open reading frame regulates the expression of inserted sequences between the second and third PDZ motifs and between the SH3 and guanylate kinase domains. These alternative splicing events may modify the protein-binding properties of the PDZ and SH3 domains. A more complex level of alternative splicing occurs at the N terminus of PSD-93, where the alternative 5′ regions are expressed in a tissue-specific manner. Thus the PSD-93 gene may contain multiple promoter regions that are differentially active in specific tissues and during specific developmental stages. Similar complex mechanisms for transcriptional regulation of the nNOS gene have been detected in human (Xie et al., 1995) and rat tissues (Brenman et al., 1996).

REFERENCES

Aoki C, Fenstemaker S, Lubin M, Go CG (1993) Nitric oxide synthase in the visual cortex of monocular monkeys as revealed by light and electron microscopic immunocytochemistry. Brain Res 620:97–113.

Bredt DS, Snyder SH (1989) Nitric oxide mediates glutamate-linked enhancement of cGMP levels in the cerebellum. Proc Natl Acad Sci USA 86:9030–9033.

Bredt DS, Snyder SH (1990) Isolation of nitric oxide synthetase, a calmodulin-requiring enzyme. Proc Natl Acad Sci USA 87:682–685.

Bredt DS, Snyder SH (1992) Nitric oxide, a novel neuronal messenger. Neuron 8:3–11.

Brenman JE, Chao DS, Xia H, Aldape K, Bredt DS (1995) Nitric oxide synthase complexed with dystrophin and absent from skeletal muscle sarcolemma in Duchenne muscular dystrophy. Cell 82:743–752.

Brenman JE, Chao DS, Gee SH, McGee AW, Craven SE, Santillano DR, Huang F, Xia H, Peters MF, Froehner SC, Bredt DS (1996) Interaction of nitric oxide synthase with the synaptic density protein PSD-95 and α-1 syntrophin mediated by PDZ motifs. Cell 84:757–767.

Bult H, Boeckxstaens GE, Pelckmans PA, Jordaens FH, Van Maercke YM, Herman AG (1990) Nitric oxide as an inhibitory non-adrenergic non-cholinergic neurotransmitter. Nature 345:346–347.

Cabral JHM, Petosa C, Sutcliffe MJ, S, R, Byron O, Poy F, Marfatia SM, Chishti AH, Liddington RC (1996) Crystal structure of a PDZ domain. Nature 382:649–652.

Cho KO, Hunt CA, Kennedy MB (1992) The rat brain postsynaptic density fraction contains a homolog of the *Drosophila* discs-large tumor suppressor protein. Neuron 9:929–942.

Daniel EE, Haugh C, Woskowska Z, Cipris S, Jury J, Fox-Threlkeld JE (1994) Role of nitric oxide-related inhibition in intestinal function: relation to vasoactive intestinal polypeptide. Am J Physiol 266:G31–39.

Doyle DA, Lee A, Lewis J, Kim E, Sheng M, MacKinnon R (1996) Crystal structures of a complexed and peptide-free membrane protein-binding domain: molecular basis of peptide recognition by PDZ. Cell 85:1067–1076.

Ferrendelli JA, Chang MM, Kinscherf DA (1974) Elevation of cyclic GMP levels in central nervous system by excitatory and inhibitory amino acids. J Neurochem 22:535–540.

Fields S, Song O (1989) A novel genetic system to detect protein-protein interactions. Nature 340:245–246.

Garthwaite J (1991) Glutamate, nitric oxide and cell-cell signalling in the nervous system. Trends Neurosci 14:60–67.

Garthwaite J, Boulton CL (1995) Nitric oxide signaling in the central nervous system. Annu Rev Physiol 57:683–706.

Garthwaite J, Charles SL, Chess-Williams R (1988) Endothelium-derived relaxing factor release on activation of NMDA rec suggests role as intercellular messenger in the brain. 336:385–388.

Garthwaite J, Garthwaite G, Palmer RM, Moncada S (1989) N receptor activation induces nitric oxide synthesis from arginine brain slices. Eur J Pharmacol 172:413–416.

Hecker M, Mulsch A, Busse R (1994) Subcellular localization and acterization of neuronal nitric oxide synthase. J Neurc 62:1524–1529.

Hunt AC, Schenker LJ, Kennedy MB (1996) PSD-95 is associated the postsynaptic density and not with the presynaptic membra forebrain synapses. J Neurosci 16:1380–1388.

Jesaitis LA, Goodenough DA (1994) Molecular characterization an sue distribution of ZO-2, a tight junction protein homologous to and the *Drosophila* discs-large tumor suppressor protein. J Cel 124:949–961.

Kiedrowski L, Costa E, Wroblewski JT (1992) Glutamate receptor nists stimulate nitric oxide synthase in primary cultures of cerel granule cells. J Neurochem 58:335–341.

Kim E, Niethammer M, Rothschild A, Jan Y, Sheng M (1995) tering of Shaker-type K^+ channels by direct interaction with PSD-95/SAP90 family of membrane-associated guanylate kin Nature 378:85–88.

Kistner U, Wenzel BM, Veh RW, Cases-Langhoff C, Garner AM, peltauer U, Voss B, Gundelfinger ED, Garner CC (1993) SAP90, presynaptic protein related to the product of the *Drosophila* t suppressor gene dlg-A. J Biol Chem 268:4580–4583.

Knowles RG, Palacios M, Palmer RM, Moncada S (1989) Formati nitric oxide from L-arginine in the central nervous system: a tran tion mechanism for stimulation of the soluble guanylate cyclase. Natl Acad Sci USA 86:5159–5162.

Kornau H-C, Schenker LT, Kennedy MB, Seeburg PH (1995) Do interaction between NMDA receptor subunits and the postsyn density protein PSD-95. Science 269:1737–1740.

Lue RA, Marfatia SM, Branton D, Chishti AH (1994) Cloning characterization of hdlg: the human homologue of the *Drosophila* large tumor suppressor binds to protein 4.1. Proc Natl Acad Sci 91:9818–9822.

Luo D, Knezevich S, Vincent SR (1993) *N*-methyl-D-aspartate-ind nitric oxide release: an in vivo microdialysis study. Neurosci 57:897–900.

Muller BM, Kistner U, Veh RW, Cases-Langhoff C, Becker B, Gunde ger ED, Garner CC (1995) Molecular characterization and sp distribution of SAP97, a novel presynaptic protein homologou SAP90 and the *Drosophila* discs-large tumor suppressor protein. J N rosci 15:2354–2366.

Raiteri M, Maura G, Barzizza A (1991) Activation of presyn 5-hydroxytryptamine-1-like receptors on glutamatergic terminals in its *N*-methyl-D-aspartate-induced cyclic GMP production in rat cere lar slices. J Pharmacol Exp Ther 257:1184–1188.

Sassoon D, Rosenthal N (1993) Detection of messenger RNA by in hybridization. Methods Enzymol 225:384–404.

Shieh BH, Zhu MY (1996) Regulation of the TRP Ca^{2+} channe INAD in *Drosophila* photoreceptors. Neuron 16:991–998.

Stevenson BR, Siliciano JD, Mooseker MS, Goodenough DA (19 Identification of ZO-1: a high molecular weight polypeptide associ with the tight junction (zonula occludens) in a variety of epithelia. J Biol 103:755–766.

Vincent SR, Hope BT (1992) Neurons that say NO. Trends Neur 15:108–113.

Willott E, Balda MS, Fanning AS, Jameson B, Van Itallie C, Anderson (1993) The tight junction protein ZO-1 is homologous to the *Dros ila* discs-large tumor suppressor protein of septate junctions. Proc Acad Sci USA 90:7834–7838.

Woods DF, Bryant PJ (1991) The discs-large tumor suppressor gen *Drosophila* encodes a guanylate kinase homolog localized at sep junctions. Cell 66:451–464.

Xie J, Roddy P, Rife TK, Murad F, Young AP (1995) Two closely lin but separable promoters for human neuronal nitric oxide synthase g transcription. Proc Natl Acad Sci USA 92:1242–1246.